Nuclear Instruments and Methods in Physics Research B 309 (2013) 95–104

Contents lists available at SciVerse ScienceDirect

Nuclear Instruments and Methods in Physics Research B

journal homepage: www.elsevier.com/locate/nimb

Registration of energy discharge in D + D → ^{4}He* reaction in conducting crystals (simulation of experiment)

E.N. Tsyganov [a,*], V.M. Golovatyuk [b], S.P. Lobastov [b], M.D. Bavizhev [c], S.B. Dabagov [d]

[a] University of Texas Southwestern Medical Center at Dallas, USA
[b] Joint Institute for Nuclear Research, Dubna, Russia
[c] North-Caucasus Federal University, Stavropol, Russia
[d] RAS PN Lebedev Physical Institute & NRNU MEPhI, Moscow, Russia

ARTICLE INFO

Article history:
Received 30 November 2012
Received in revised form 29 December 2012
Accepted 12 January 2013
Available online 3 April 2013

ABSTRACT

The experiment on registration of low-energy electrons which occur after the fusion reaction of two deuterons in the palladium crystal at very low excitation energies was modeled using Monte Carlo simulations.

1. Introduction

The first two elements of our Universe and their stable isotopes of hydrogen and helium were produced in the first minutes of the Universe, after the so-called "Big Bang". A small amount of lithium, the third element in the periodic table, was also made at this time. However, the bulk of the lithium, and beryllium, and boron elements were formed from heavier elements in the process of disintegration of these elements in interstellar space, under the influence of cosmic radiation. All the chemical elements that make up the Earth and us from carbon to uranium, as is commonly believed, originated in nuclear processes inside the "burnt" stars during their long evolution.

Our life on Earth was made possible due to the heating from the nearest star, which we call the Sun. The Sun is a relatively young star, with a long lifetime. Solar energy is due to the synthesis of helium from hydrogen, the nuclear process that occurs in the depths of the star and ensures our existence.

At the present time, mankind has come to a stage of development, when the struggle for energy resources has become particularly urgent. In the next 100–200 years, all known chemical resources will be close to exhaustion, which has a detrimental effect on our future development. All the known renewable energy resources cannot meet the needs of human progress. The problem is exacerbated by the fact that the chemical energy is bound by the so-called greenhouse effect, i.e. the excess in the atmosphere of carbon dioxide.

Talk about the transition to the use of nuclear energy has been going on for a long time. As it turned out, nuclear energy, based on the use of fissionable nuclear material, is not a lasting solution to the problem, as the stocks of these materials are not infinite. Reactor safety, based on the process of nuclear fission, must be much more reliable, as has been shown by several recent accidents at nuclear power plants. Disposal of nuclear waste for a very long time is still a virtually unsolved problem.

For a long time there has been talk about transitioning to a process of controlled nuclear fusion. Initial expectations that this problem would be solved soon did not materialize. Technical difficulties maintaining superhot plasmas (10^7–10^9 C) and the destructive effect of gigantic neutron fluxes produced by thermonuclear reactions are pushing the solution of this problem to a more distant and uncertain future.

Recently, the hope, or even assurance, that the problem of nuclear fusion can be solved quite differently has been aroused.

Calorimetric measurements of samples of palladium saturated with deuterium (a group of McKubre, as well as several other groups) indicate that, the so-called cold fusion of two deuterium nuclei to form ^{4}He* with the concurrent release of energy of 24 MeV [1] occurs under these conditions. These experiments have been conducted for nearly 23 years, and are still either completely rejected by the working community of nuclear physicists, or met with a large dose of skepticism. Two main objections raised by nuclear physicists against the experiments of the McKubre group and other similar experiments are clustered around the apparent violation of the second law of thermodynamics by this process and the fact that in these experiments there are virtually no nuclear reaction products, except ^{4}He.

It was shown in papers [2,3] that the results of these experiments are not contrary to the fundamental laws of physics. We will show below that the experiments at accelerators at low energies directly indicate the need for the existence of this phenomenon, which was first observed by the unexpected heating during the reaction in palladium saturated with deuterium. The virtual absence of nuclear products in the reaction of cold fusion of deuterons can be explained

* Corresponding author. Tel.: +1 972 709 5436.
E-mail address: edward.tsyganov@coldfusion-power.com (E.N. Tsyganov).

0168-583X/$ - see front matter © 2013 Elsevier B.V. All rights reserved.
http://dx.doi.org/10.1016/j.nimb.2013.01.077

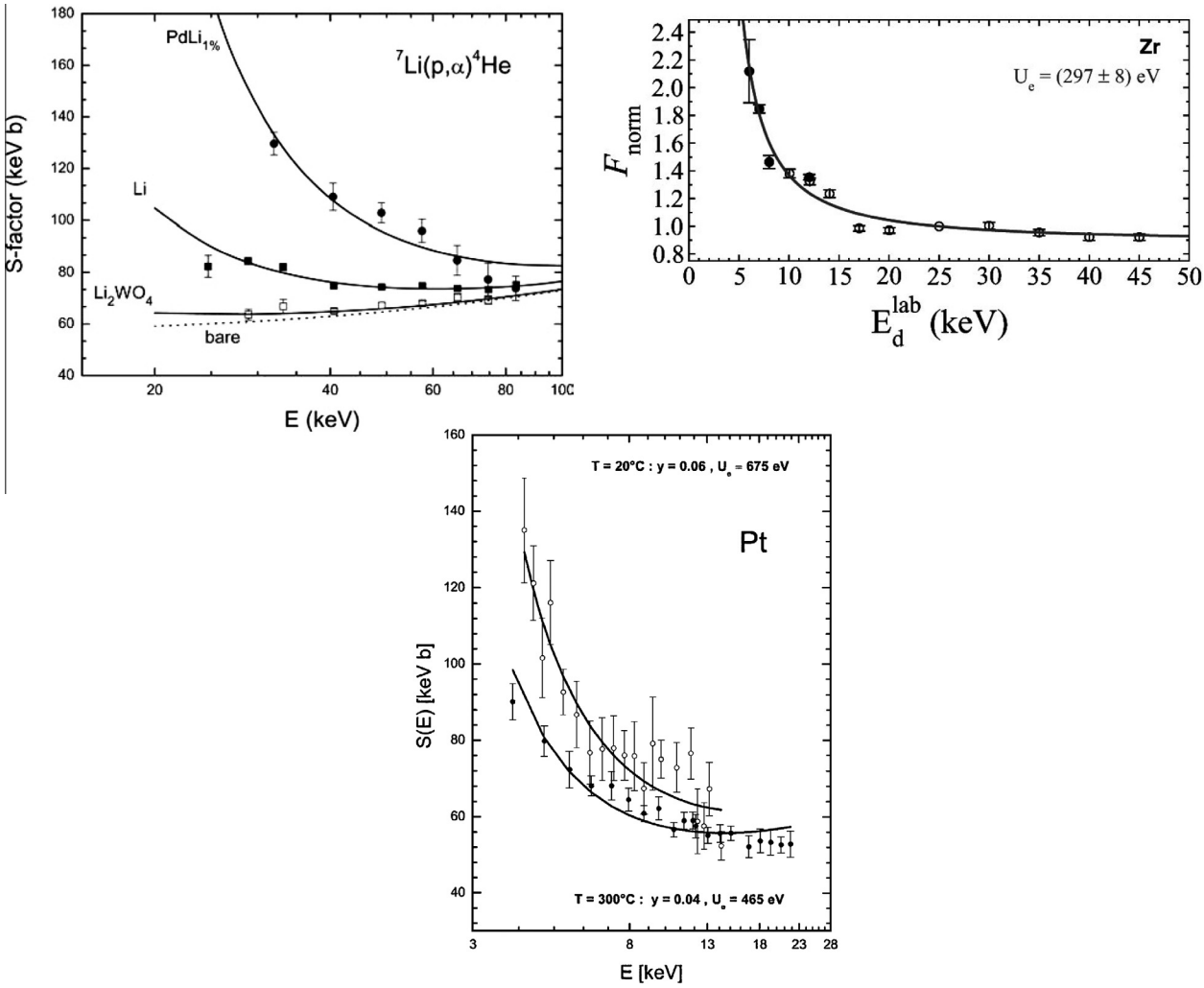

Fig. 1. Upper panel: left – experimental data [6], showing the energy dependence of the S-factor for sub-threshold nuclear reaction on the aggregate state of matter that contains the nucleus ^{7}Li. Right – similar data [7] for the reaction DD, when the target is placed in a crystal of zirconium. The data are well described by the introduction of the screening potential of about 300 eV. Lower panel – the data for the reaction DD [8], when the target is implanted in a crystal of platinum. The data are well described by the introduction of the screening potential of about 675 eV.

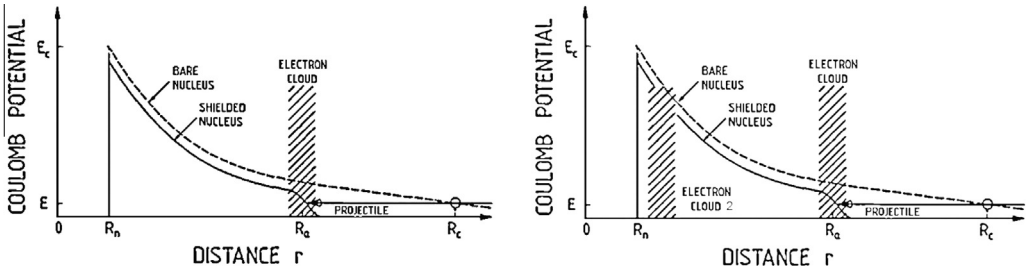

Fig. 2. Left panel – sketch from the paper of Assenbaum and others [4], illustrating electron screening in a fusion process. Until the distance R_a, the projectile particle is not repelled by the target nucleus. If the electron orbit of the target could be (hypothetically) moved toward the target nucleus, the strength of the Coulomb barrier could be drastically lowered (right panel).

by the decreasing of the rate of nuclear decay of the intermediate nucleus ^{4}He* with decreasing energy of its excitation. In this case, the energy of the reaction is released by virtual photons. Thus, this is a new phenomenon, which may be of great practical importance. In addition, the study of so-called "glow discharge" of the excited ^{4}He* nucleus may clarify the mechanism of packaging of the nuclear system and suggest a new approach to the study of the chromodynamical nature of nuclear forces [3].

2. Fusion reactions in collisions of atoms in crystal environments

In contrast to the collision of bare nuclei, it is necessary to modify the formula for the probability of penetration through the potential Coulomb barrier for the collision of atoms, because the atomic electrons screen the repulsive effect of a nuclear charge. In the so-called Born–Oppenheimer approximation, such a

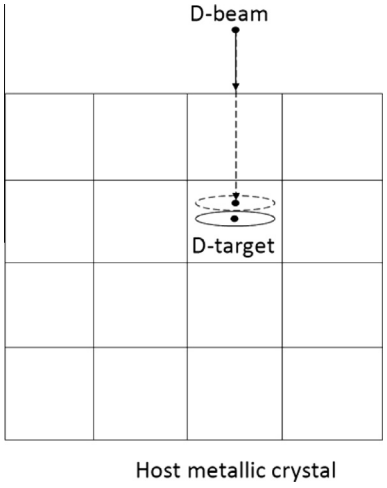

Fig. 3. Sketch of the Gran Sasso experiments of fusion elements when the target is embedded in a conductive crystal.

modification for the atom–atom collisions has been performed in Assenbaum and others [4]. Under this approach, it was shown that the so-called "screening potential" serves as effective additional energy for the collisions of nuclei in the center of mass system. Experimental data can be well described by the introduction of only one parameter – the screening potential, which for deuterium in metals is about an order of magnitude greater than is the case for collisions of free atoms. Apparently, this approach is equivalent to taking into account the thickness of the potential barrier for calculation of the quantum–mechanical penetration probability through potential barriers developed earlier by Zeldovich and Gershtein [5]. The Assenbaum approach is presumably valid until this screening potential is much less than the peak value of the barrier potential.

The experimental results that shed unexpected light on this problem are presented in works by Rolfs [6], Czerski [7] and Raiola [8]. A survey of papers on this subject is contained in the article by Bogdanova [9]. In these studies it was shown that sub-barrier cross sections of element synthesis depend very strongly on the physical state of the matter in which the target atoms are embedded. Fig. 1 shows the experimental data [6–8], demonstrating the dependence of the astrophysical factor S(E) and cross sections of the synthesis of elements for sub-threshold nuclear reaction on the aggregate state of matter that contains the target nucleus.

The distance of convergence of the two deuterium atoms in one crystalline cell under these circumstances is an order of magnitude smaller than the size of a deuterium atom. It must be noted that the physical nature of the phenomenon of increasing fusion cross section of elements placed in the crystal lattice of conductive crystals is not yet fully elucidated.

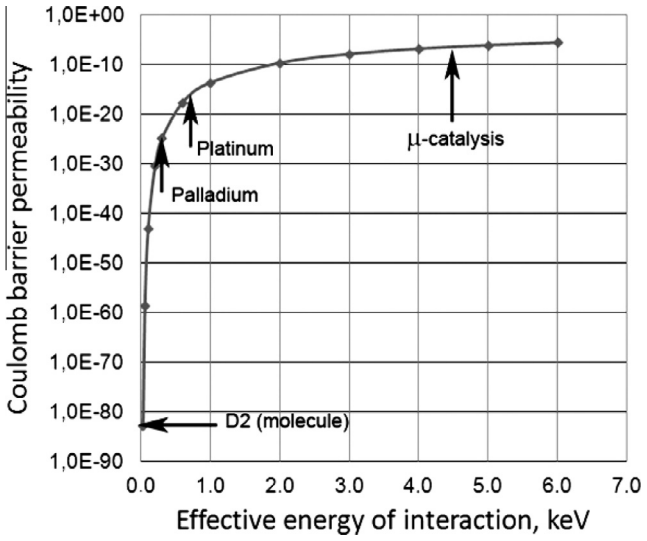

Fig. 5. Permeability of the Coulomb barrier for DD fusion vs electron screening potential ("effective energy of interaction").

Table 1
Rate of DD fusion in a single niche of crystallographic cell.

Crystal	Screening potential, eV	Oscillation frequency ν, s^{-1}	Barrier permeability $e^{-2\pi\eta}$	Rate of DD fusion λ, s^{-1}
Palladium	300	0.74×10^{17}	1.29×10^{-25}	0.95×10^{-8}
Platinum	675	1.67×10^{17}	2.52×10^{-17}	4.21

Table 2
Series of hydrogen spectra based on Rydberg formula.

n_1	n_2	Name of Series	Converge toward
1	$2 \to \infty$	Lyman	91.13 nm (UV)
2	$3 \to \infty$	Balmer	364.51 nm (Visible)
3	$4 \to \infty$	Paschen	820.14 nm (IR)
4	$5 \to \infty$	Brackett	1458.03 nm (Far IR)
5	$6 \to \infty$	Pfund	2278.17 nm (Far IR)
6	$7 \to \infty$	Humphreys	3280.56 nm (Far IR)

As we mentioned earlier, the effect of electron screening in the fusion process was quite careful considered by Assenbaum, Langanke and Rolfs [4]. Fig. 2 (left panel) illustrate the physics of the process.

In 1960 Zeldovich and Gershtein [5] considered the permeability of the Coulomb barrier and found that it is strongly depended on the orbit radius of the screening electron:

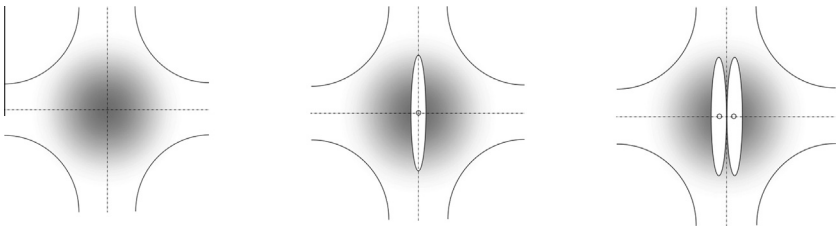

Fig. 4. Sketch of the niches in metallic crystalline cells. A shadow area schematically represents free electron clouds. Left – an empty crystalline niche, the middle – a niche, filled with one contaminant deuterium atom. Right – a niche, filled with two deuterium atoms. The fusion process is only possible when two deuterium atoms met in the same crystalline niche. A simple cubic structure is used in the sketch just for didactical purposes.

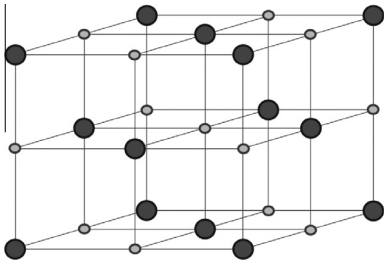

Fig. 6. The structure of the fcc crystal lattice. Large circles denote the atoms of the crystal lattice, small circles marked off the so-called octahedral centers (O) with a minimum of electrical potential.

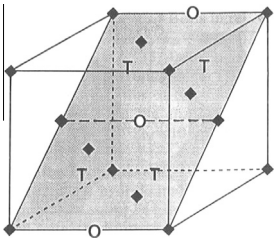

Fig. 7. Diagonal plane in the structure of fcc [12]. Octahedral positions (O) and tetrahedral positions (T) of potential wells are presented.

$$B = \exp\left\{-\frac{2}{\hbar}\int_{x_1}^{x_2}\sqrt{2M(U(x)-E)}dx\right\} = \exp\left\{-\frac{2}{\hbar}\sqrt{2M\overline{U}}(x_2-x_1)\right\}$$

They considered the possibility of reducing the radius of the electron orbits of fusing atoms using deuterium under very high pressure ("dreams" of piezo-fusion). Unfortunately, the necessary pressure happens to be so high, that it was completely impractical.

Fig. 3 is a sketch of the Gran Sasso experiments. A beam of several keV deuterons bombards deuteron atoms previously implanted in the matrix of a crystal or of an amorphous material. At these low energies the naked deuterons, when entering the crystalline matter, acquire orbital electrons and move inside the crystal as whole atoms, and an atom–atom interaction takes place in the cell of the host material. The process of acquiring an orbital electron happens when the velocity of the deuteron in the matter is lower than the Bohr velocity of an electron in a hydrogen atom. For deuterons this threshold is 50 keV.

Cross-section of this reaction manifests that so-called electron screening potential is high in metallic crystals, of the order of 300–700 eV. This means that before the fusion reaction has taken place, both deuteron atoms are approaching each other without repulsion to a distance less than one tenth of the size of the free deuterium atoms. In other words, before the fusion reaction has take place, both electron orbits of interacting deuterium atoms in the crystalline cell have elongated shapes, as shown schematically in Fig. 3. This reaction is still the fusion-in-flight, a single encounter of two atoms. These fusion reactions were identified in the Gran Sasso experiments by the normal radiation products of the hot DD fusion [d(d, p)t)].

In the explanation of the cold fusion process presented in paper [3] it was reasonably supposed that two deuterium atoms, when they implanted in the same crystalline niche, have the same elongated electron orbits, which are strictly oriented in the crystalline cell. In paper [3], parameters of the electron screening potentials from the Gran Sasso and following experiments were applied to the McKubre experiments. The reasonable assumption was made that the changes of shape of an electron orbit of a bullet deuterium atom in Gran Sasso experiments are quite fast during their travel in the crystalline cell. We do believe so, because the speed of the bullet deuterium atoms in Gran Sasso experiments is much slower than the electronic processes in the crystal. If it is not completely true, even larger screening potential should be applied for cold fusion.

Fig. 4 provides a sketch of the niches in metallic crystalline cells. A shadow area schematically represents free electron clouds. The fusion process is only possible when two deuterium atoms met in the same crystalline niche.

Fig. 5 shows a graph of permeability of the potential Coulomb barrier for the D + D → ^{4}He* reaction on the electron screening potential (effective energy of interaction).

The possibility of a process analogous to the well-known process of muon catalysis, when instead of μ-meson exchange catalysis the rapprochement of two deuterons is the effect of conduction electrons and the lattice of the metal crystal, was considered in [3],

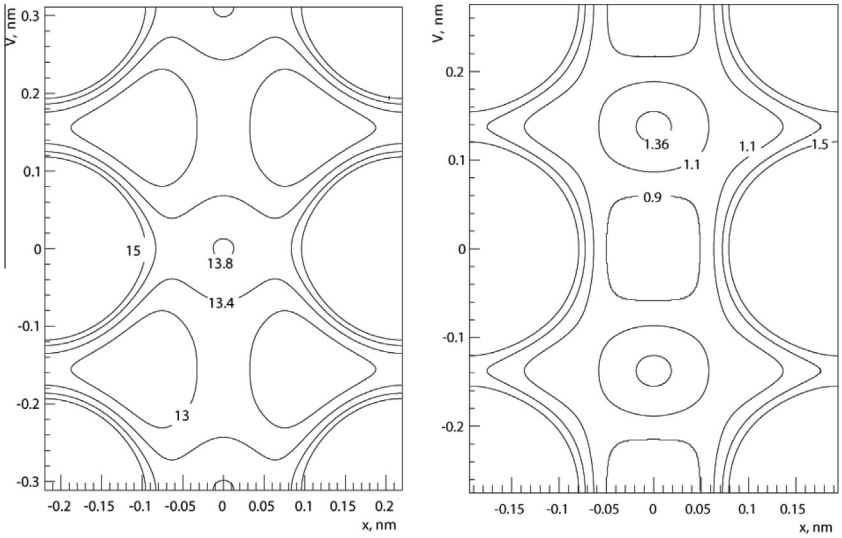

Fig. 8. Potential isolines within the fcc cell (diagonal plane) in the case of titanium (left) and palladium (right) on the DFT model. The potential values for contour isolines are given in volts.

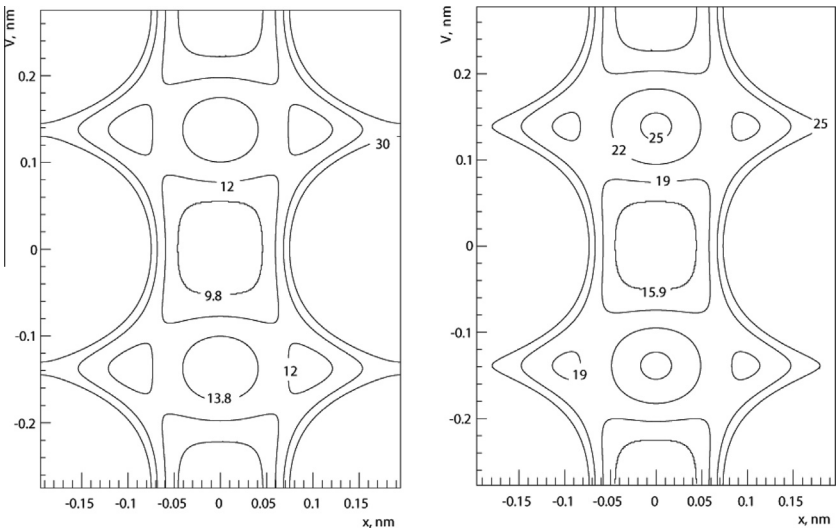

Fig. 9. Potential isolines within the cell fcc (diagonal plane) in the case of palladium crystal (left) and platinum (right) in the Molière approximation. The potential values for contour isolines are given in volts.

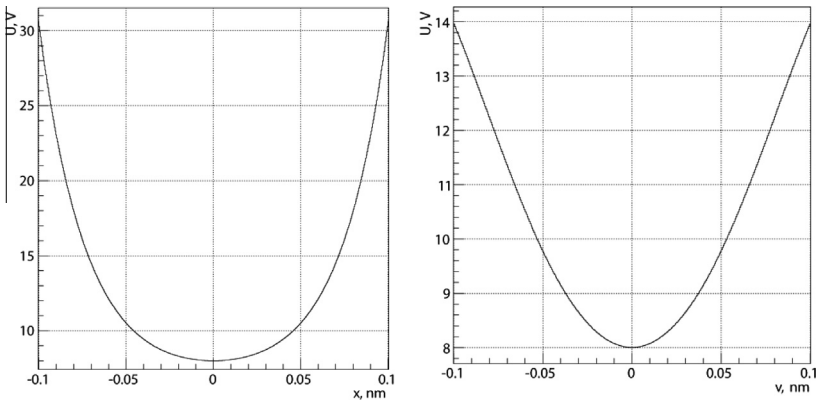

Fig. 10. Profiles of the potential in O-center in palladium crystal in the X-direction (left) and in the V-direction (right), Molière approximation.

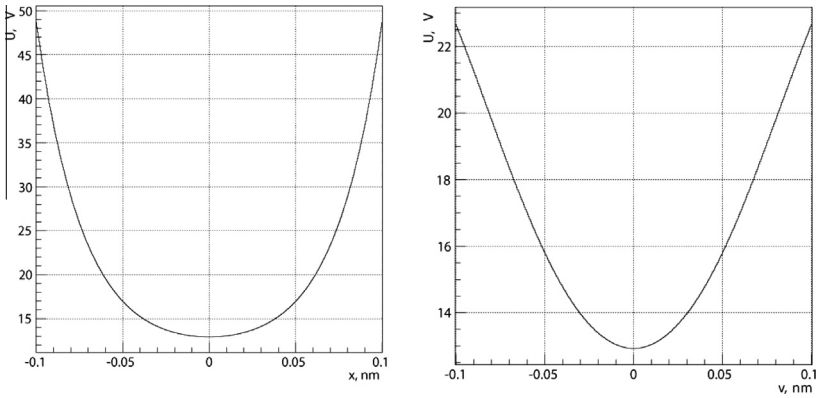

Fig. 11. Profiles of a potential in O-center in platinum crystal in the X-direction (left) and the V-direction (right), Molière approximation.

where the calculation of DD fusion reaction rate in the crystals of palladium and platinum was done. In the case of palladium [7], the screening potential was taken to be 300 eV, the same as in the case of zirconium. For platinum the screening potential is 675 eV [8]. A screening potential of 3–6 keV approximately corresponds to μ-catalysis for DDμ.

It is very clear from the graph in Fig. 5 that the dependence of the DD fusion reaction rate, which is proportional to the probability of penetration of the deuterons through the barrier, increases drastically with increasing electron screening potential. The resulting rate of DD fusion located in a single niche of a crystallographic cell of palladium and platinum is presented in Table 1.

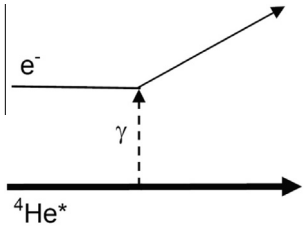

Fig. 12. Diagram of the processes that ensure thermalization of DD-fusion reactions in crystals. Virtual photon is emitted by compound nucleus $^4He^*$.

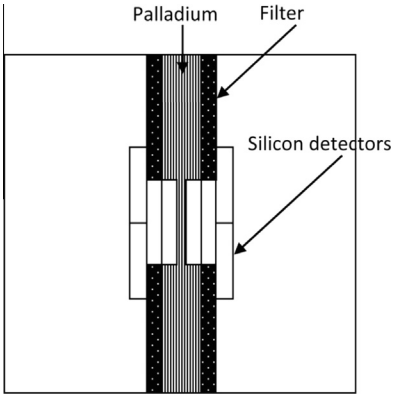

Fig. 13. The scheme of the two-side experiment is presented. Several semiconductor silicon detectors are located on both sides of the palladium crystal and are included in the coincidence.

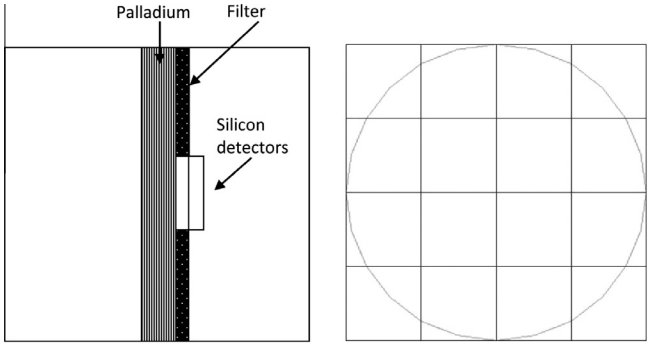

Fig. 14. The one-sided scheme of the experiment is presented. Several semiconductor silicon detectors located on one side of the palladium and included in the coincidences. Left – side view, right – the relative position of the aperture and detectors.

It is usually accepted, that at the ground state of the hydrogen atom the shape of the electron orbit is round. However, the free electron cloud in a metallic crystal could distort the electron orbit of a contaminant atom with the application of very small excitation energy, of the order of several eV. Well known chemical catalysis processes are based on this phenomenon. Spectra of hydrogen atoms, containing elliptical atomic orbits, were first proposed by Rydberg with his famous formula in 1888: $1/\lambda = R\,[(1/n_1^2) - (1/n_2^2]$. Table 2 presents a series of hydrogen spectra based on Rydberg formula.

3. Crystalline structures and cell potentials

The most common crystalline structures are known as simple cubic (sc or cP), body centered cubic (bcc or cI), face centered cubic

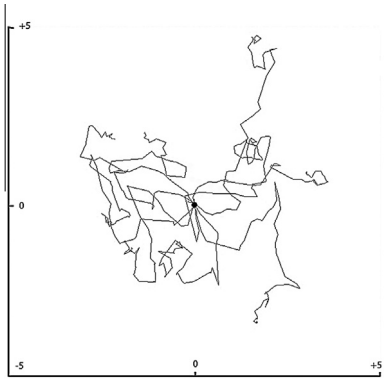

Fig. 15. Example trajectories of 10 emitted electrons with energy of 60 keV. Electrons emitted isotropically from a single point in palladium (in the plane XY). Dimensions are in micrometers.

(fcc or cF), and hexagonal. Palladium and platinum are both characterized by the fcc structure. Let note that there are no metallic crystals with simple cubic structure, and in our previous considerations we have used it just for didactical purposes. Moreover, in such a structure the only potential niche for contaminants is placed in the center of the cube. As below shown, for heavy metals like palladium and platinum the main potential niches are somewhat similar to those of simple cubic structures.

To date, there is no distinct quantum–mechanical theory of solids, even for the case of such highly ordered systems as crystals. Complex calculations of the electron shells of different atoms have only been performed relatively recently, about 50 years ago. The existence of even the simplest molecule – hydrogen (H_2) – fundamentally depends on the relative electron spin orientation of two H atoms considered (ortho-hydrogen and para-hydrogen). It would be naive to think that the cell structure of a crystalline platinum consisting of hundreds of "players" could actually be calculated theoretically by only means of relevant rules of thumb without the use of experimental data.

As above mentioned, the experiments at the Gran Sasso Laboratory [6,8] and in Berlin [7] carried out in 2002–2009, that have been repeatedly cross-checked by these two large international teams, led to the establishment of an interesting observation. The so-called electronic screening potential in the synthesis reaction (e.g., in the case of DD) dramatically increases when the reaction occurs in the medium of a conducting crystal. On the contrary, this enhancement is absent for reactions in a semiconductor, insulator or amorphous body. In these cases, the electronic screening potential is virtually identical to the values obtained for collisions of free atoms. It should be underlined that the effect of an increase of the electron screening was first recorded in a hot fusion experiment, and protons were emitted from the $D + D \rightarrow {}^3H + p$ reaction. Regardless of the difference of proton emission, for these two processes the permeability of the Coulomb barrier is expressed with the same quantum–mechanical expression.

Already in 2006, Claus Rolfs noted [6] that the large electronic screening potential indicates the possibility of convergence of deuterium interacting each other without the Coulomb repulsion at the distance much less than the canonical dimensions of these atoms. Unfortunately, the studies did not pursue this idea further applying it, for instance, for the so-called cold fusion case. To make such a generalization, we should assume that the atoms involved in the reaction are arranged in the same potential niche of a metallic crystal cell, and set $E_{kin} = 0$ in the expression for the effective potential $E_{eff} = E_{kin} + U_e$.

Calculations of the reaction rate reported in [2] are based explicitly on the experimental data [7,8], and do not depend on

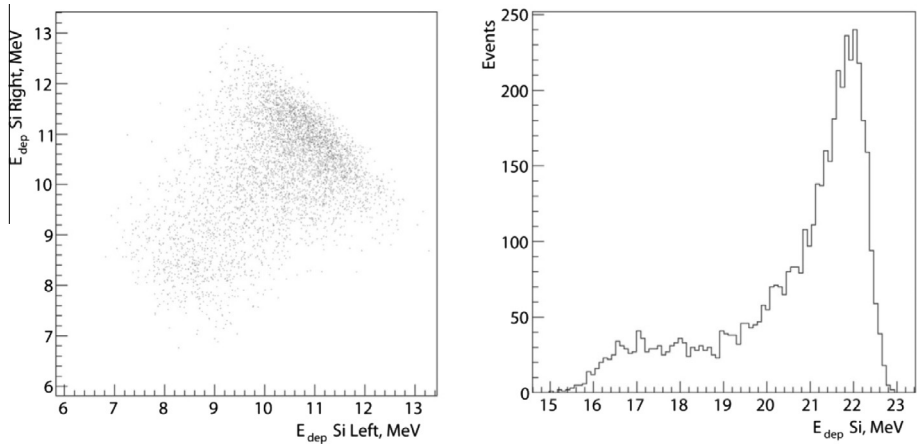

Fig. 16. Left – the energy released by 6 keV electrons in detectors on the left and the right of a palladium foil with a thickness of 0.1 micrometers. Right – the total energy released in this case.

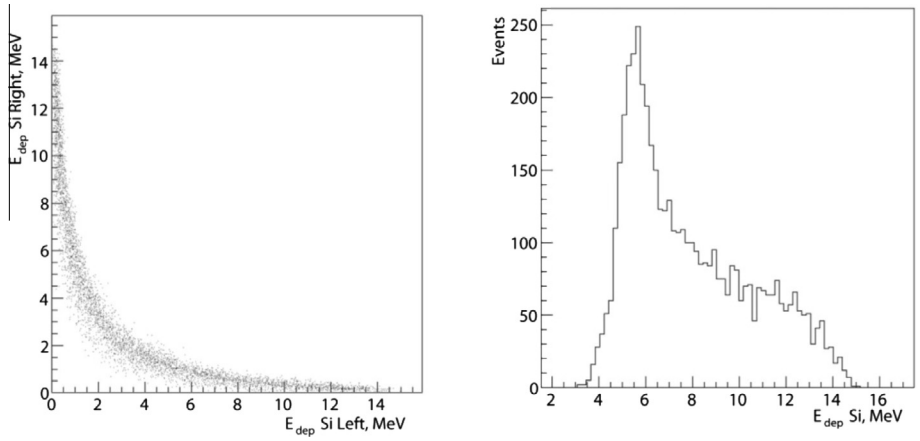

Fig. 17. Left – the energy released by 6 keV electrons in detectors on the left and the right of a palladium foil with a thickness of 1 μm. Right – the total energy release.

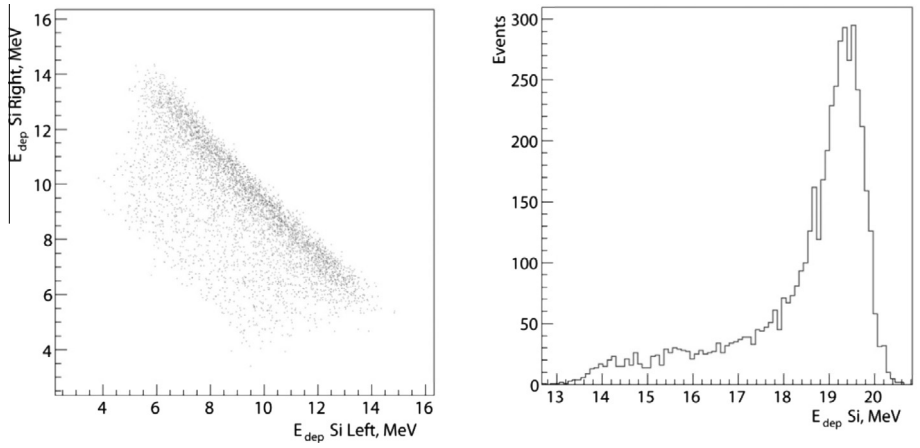

Fig. 18. Left – the energy released by 60 keV electrons in detectors on the left and the right of a palladium foil with a thickness of 5 μm. Right – the total energy release.

the structure of the potential niches in the metal crystal, or on detailed mechanism of deformation of the electron shells for deuterium atoms. However, the study of the configuration of such niches may help further to understand the mechanism of cold fusion.

Let calculate the electrical potentials for various fcc structure cells.

3.1. Thomas–Fermi and DFT models for the potential evaluation

As known, interaction potential in the Thomas–Fermi model is written as

$$V(r) = \frac{Z_1 Z_2 e^2}{r}\phi(r/a) \quad (1)$$

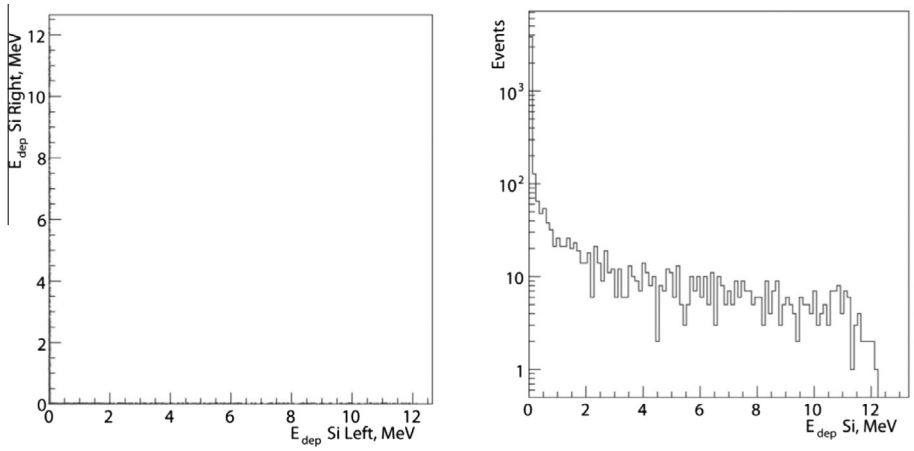

Fig. 19. Left – the energy released by 6 keV electrons in detectors on the left and the right of a palladium foil with a thickness of 1 μm. Right – the total energy release.

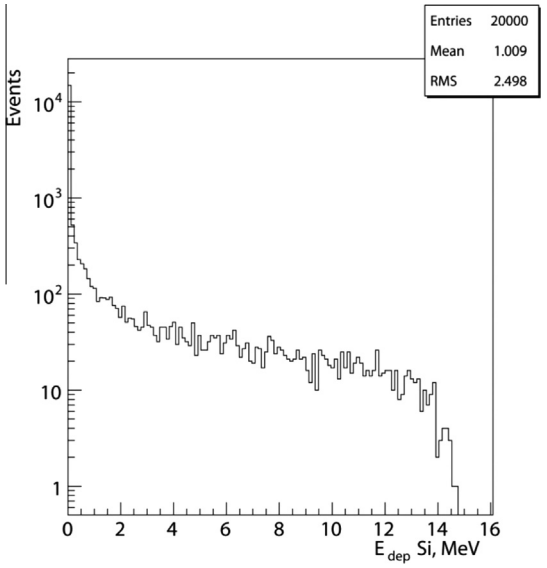

Fig. 20. The release of energy by 60 keV electrons in the detectors located on one side of the palladium (palladium foil thickness was taken equal to 20 μm). About 75% of the events that have been simulated are completely absorbed in the palladium. The spectrum is cut off by about 14 MeV due to re-scattering of a certain fraction of electrons in the palladium for 180°.

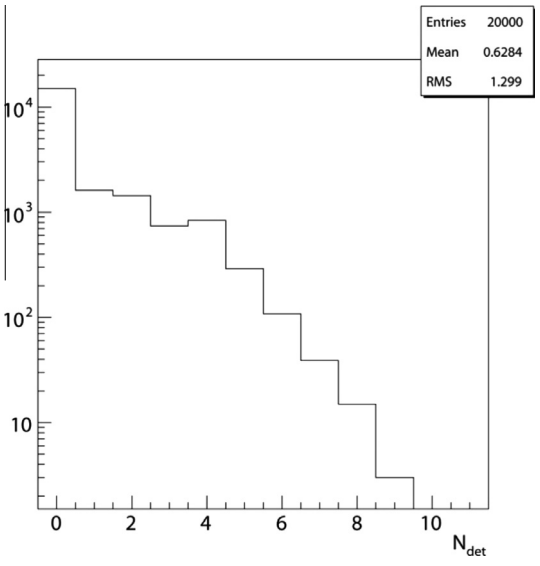

Fig. 21. The distribution of events by the number of triggered detectors for the one-side option of the detectors in the case of 60 keV. The threshold of the detectors was set at 100 keV.

where the screening function $\phi(r/a)$ could be calculated within various approximations. One of wide used approximation known as a Molière approximation [10] (for details see [11]) represents a sum of exponents that simplifies its use:

$$\phi(r/a)=\sum_{i=1}^{3}\alpha_i\exp\left(-\tfrac{\beta_i r}{a}\right)\{\alpha_i\}=\{0.1,0.55,0.35\},\ \{\beta_i\}=\{6.0,1.2,0.3\} \qquad (2)$$

with the screening length a in the case of an isolated atom (Z_2) and interaction with fully ionized ions (Z_1)

$$a=0.8853\,a_1 Z_2^{-1/3} \quad , \qquad (3)$$

where $a_1 = 0.529$ Å is the Bohr radius. In our case, $Z_1 = 1$, $Z_2 = 46$ (palladium) and 78 (platinum).

Approximation of Density Functional Theory (DFT) is further development of Hartree–Fock theory and apparently is the most appropriate method of calculation in solid state physics. For simplicity in the description of the most common characteristics of the potentials in the crystal cell of heavy metals we limited ourselves by the Molière approximation. We have also performed the calculations in accordance with the DFT and compared our results with the work of Ichimaru [12]. A book "The Fundamentals of Density Functional Theory" written by Eschrig [13] contains detailed mathematical discussions on the DFT.

3.2. The results of calculations for the fcc structure

The crystal fcc structure is presented in Fig. 6. Large circles denote the atoms of the crystal lattice, small circles marked by the so-called octahedral centers (O) with a minimum electrical potential. It is easy to see that when you move the reference center from the upper-left cell of the lattice to the middle atom of the cell by a half cell constant in the *X*- and the *Y*-directions, i.e. $(X + a/2, Y + a/2)$, the structure of the entire cell is repeated itself, with the central O center becoming one of the edge. This means that all of the O-centers in this structure are identical.

Fig. 7, taken from [12], offers pleasant view of the structure of potential octahedral O and tetrahedral niches T, located on the diagonal plane in the structure of fcc. We will denote the horizontal direction in the cell as *X*, and the direction along the diagonal plane as *V*.

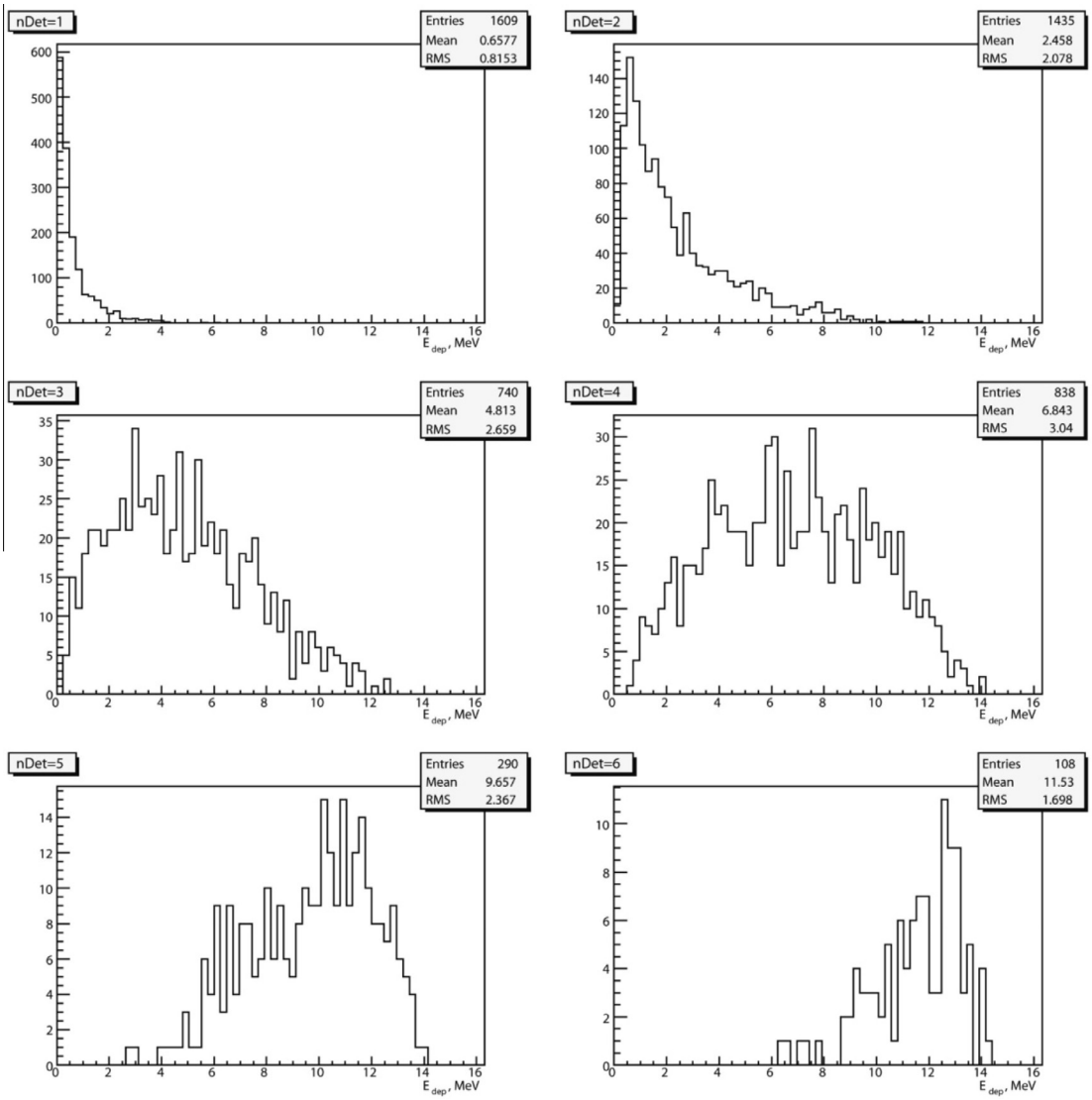

Fig. 22. The distribution of the total energy released by 60 keV electrons for the case when the detectors are located on one side of a palladium foil with a thickness of 20 μm. The different histograms correspond to the different coincidence multiplicity of the detectors. The threshold of the detectors was set at 100 keV.

To get a realistic potential distribution within a single crystal cell, even with the spatial distribution of the potential of a single atom, one should place the cell in a group of a large number of similar cells. This is necessary in order to avoid distortion of the results arising from edge effects. We have calculated a few conglomerates of crystal cells (single cell, clusters $3 \times 3 \times 3$, $5 \times 5 \times 5$, $7 \times 7 \times 7$) and came to the conclusion that the central cell of the cluster $7 \times 7 \times 7$ quite accurately reproduces potentials of "infinitely large" cluster.

Despite some discrepancy in the absolute values of potentials in the case of DFT model and Molière approximation, the general behavior of the potentials in both models satisfactory agreed. The role of T-centers gradually disappears when we move to the heaviest fcc crystals (Figs. 8–11).

4. The experiment

In this study, we examined the possibility of detecting the reaction of cold fusion in crystals, based on the hypothesis [3] that with decreasing excitation energy of the compound nucleus, the $^4He^*$ decay rate of this nucleus with the emission of nuclear products is inversely proportional to the excitation energy. In this case, the main mechanisms for the transfer of the difference of the binding energy of the nucleons in two deuterium nuclei and in ^4He (24 MeV) are processes involving virtual photons which start to play the major role. Fig. 12 shows one of these processes.

In this process, the energy of the transition of a compound nucleus $^4He^*$ to the ground state of ^4He is released through a series of virtual photons which transfer their energy to the surrounding electrons of the crystalline lattice.

Unfortunately, the calorimetric approach does not come close to providing a clear understanding of the DD cold fusion process. Additional experiments that can explain the mechanism of energy transfer of DD fusion to the crystal lattice without the nuclear decay of the composite system $^4He^*$ are required.

Figs. 13 and 14 below provide an overview of the experimental geometry, which would give additional information about the process of DD cold fusion in the crystals.

As noted above, the metallic crystals with the conduction electrons and the effect of their lattice can strongly modify the potential barrier effect. The effective screening radius in this case can be an order of magnitude smaller than the radius of the orbital

electrons of the colliding nuclei. Accordingly, the energy of the electrons from the "discharge" of an excited compound nucleus via virtual photons [2,3] may be an order of magnitude greater than in the case of a collision of free atoms. We have performed calculations for two energies of emission of electrons, 6 keV and 60 keV. This corresponds to two values of the screening potential in the DD interaction for free atoms (27 eV) and for the atoms in the conducting crystal lattice (about 300 eV for palladium crystals).

In the case shown in Fig. 13, several semiconductor silicon detectors are mounted on both sides of a palladium crystal. To reduce the accidentals, they are included in coincidence with a certain minimal threshold, and in the case of the coincidence their signals are summed. Detectors are placed with the n-side toward the radiation source and the thickness of the passive part (n-implantation) is not more than 0.02 μm. To reduce the absorption of emission electrons in the material, the air is pumped out from the surrounding volume. The estimated energy resolution of the detectors is 10 keV, with time resolution of about 2 ns [14].

To reduce the thickness of palladium, which is not a detecting element, a working sample of palladium foil is thinned by etching. The thickness of the thin wall is 1–5 μm. The thick part of the palladium element is covered by the filter.

It must be noted that from a single DD fusion event a few 100 electrons are emitted, their total energy is 24 MeV, and the identification of such an event will not present much difficulty. For further study of this phenomenon, we propose using pixelated detectors with high spatial resolution.

At the preliminary stage of the experiment, it is planned to carry out measurements by recording the emission electrons from only one side of the palladium. A schematic of the experiment in this formulation is shown in Fig. 14. 16 semiconductor silicon detectors are located on one side of the palladium and included in the coincidences.

We have to clarify here that for the all proposed measurements the density of deuterium contamination in palladium foil must be by many orders of magnitude lower than in experiments [1], where fusion effect was detected by a heat deposition. In our approach the rate measurements will be performed by detecting fusion events one by one. We plan to increase deuterium-in-palladium contamination gradually, until the counting rate will reach some suitable level.

5. The results of simulation

The total energy, to be recorded by the detectors, was calculated by the Monte Carlo model (GEANT4) [15]. For a detailed simulation of low-energy electromagnetic interactions the Livermore Physics models [16] (G4EmLivermorePhysics) from the package GEANT4 were used. These models use the databases Livermore EPDL and EEDL.

It is assumed that a fusion event produces up to several hundred electrons of 60 keV (or up to several thousand electrons of 6 keV) with the total energy of 24 MeV in a relatively short time (about 10^{-15} s). Palladium foil is not an active detecting element, so the energy of the electrons resulting from DD fusion absorbed in the foil disappears from the measurement process. The calculations optimize the thickness of the palladium foil and the geometry of the detectors.

The results of simulations are presented in Figs. 15–22.

6. Discussion

In the case of 60 keV electron emissions and a thickness of the palladium foil of 5 μm, recording events in left–right coincidence, apparently, does not present much difficulty. Thus, when a single detector threshold is placed at 100 keV, the probability of right–left coincidence in the proposed geometry is about 97%. In the case of electrons with energy of 6 keV, the probability of right-left coincidence virtually disappears, even for a thickness of 1 μ palladium. Nevertheless, reliable event detection can be made by multiple coincidences of detectors placed on one side. In the proposed geometry for the case of energy of 6 keV and the thickness of 1 μ palladium, two or more detectors will be triggered with a frequency of only about 7%. In this case, finer partitioning of the detectors will increase the frequency of operation and reliable recording of a one-sided ("surface") of the reaction.

For an easier case where the detectors are located on one side of the palladium (in the case of a thick palladium sample), the maximum detected energy is approximately half the energy of a $^4He^*$ discharge. In our opinion, this will be conclusive evidence of the transfer of energy of an excited compound nucleus $^4He^*$ to the lattice crystal by virtual photons.

Acknowledgments

The authors are very grateful to Dr. A.M. Taratin for fruitful discussions. The authors also thank S.V. Kashigin for help in choosing the design of semiconductor detectors.

References

[1] M.C.H. McKubre, F. Tanzella, P. Tripodi, et al., in: F. Scaramuzzi (Ed.), Proceedings of the 8th International Conference on Cold Fusion Lerici (La Spezia), 2000, Italian Physical Society, Bologna, Italy, 2001, p. 3;
M.C.H. McKubre, in: P.L. Hagelstein, S.R. Chubb (Eds.), Condensed Matter Nuclear Science: Proceedings of The 10th International Conference on Cold Fusion, Cambridge, MA, USA, 21–29 Aug., 2003, World Sci., Singapore, 2006;
Review of Experimental Measurements Involving DD Reactions, presented at the Short Course on LENR for ICCF-10, Aug. 25, 2003.
[2] E.N. Tsyganov, Preprint LNF–11/03 (P), April 6, 2011.
[3] E.N. Tsyganov, Phys. At. Nucl. 75 (2) (2012) 153–159.
[4] H.J. Assenbaum, K. Langanke, C. Rolfs, Z. Phys. A – At. Nucl. 327 (1987) 461–468.
[5] Ya. B. Zeldovich, S.S. Gershtein, Usp. Fiz. Nauk LXXI (4) (1960) 581 (in Russian).
[6] C. Rolfs, Enhanced electron screening in metals: a plasma of the poor man, Nucl. Phys. News 16 (2) (2006).
[7] A. Huke, K. Czerski, P. Heide, G. Ruprecht, N. Targosz, W. Zebrowski, Phys. Rev. C 78 (2008) 015803.
[8] F. Raiola, (for the LUNA Collaboration), B. Burchard, Z. Fulop, et al., J. Phys. G: Nucl. Part. Phys. 31 (2005) 1141;
F. Raiola, (for the LUNA Collaboration), B. Burchard, Z. Fulop, et al., Eur. Phys. J. A27 (2006) 79.
[9] L.N. Bogdanova, in: Proceedings of International Conference on Muon Catalyzed Fusion and Related Topics, Dubna, June 18–21, 2007, JINR, E4, 15-2008-70, pp. 285–293.
[10] G.Z. Molière, Naturforsh. A 2 (1947) 133.
[11] D.S. Gemmel, Rev. Mod. Phys. 46 (1974) 129.
[12] S. Ichimaru, S. Ogata, A. Nakano, J. Phys. Soc. Jpn. 59 (11) (1990) 3904–3915.
[13] H. Eschrig, The Fundamentals of Density Functional Theory, Institute for Solid State and Materials Research Dresden, and University of Technology, Dresden, 2003.
[14] S. Agostinelli et al., Nucl. Instr. Meth. A506 (2003) 250.
[15] Recent Improvements in Geant4 Electromagnetic Physics Models and Interfaces. Joint International Conference on Supercomputing in Nuclear Applications and Monte Carlo 2010 (SNA and MC2010), Hitotsubashi Memorial Hall, Tokyo, Japan, October 17–21, 2010.
[16] G4EmLivermorePhysics Package.